Hemodynamic Assessment of Virtual Surgery Options for a Failing Fontan Using Lumped Parameter Simulation

CM Haggerty[1], DA de Zelicourt[1], KS Sundareswaran[1], K Pekkan[2], B Whited[1], JR Rossignac[1], MA Fogel[3], AP Yoganathan[1]

[1]Georgia Institute of Technology, Atlanta, GA, USA
[2]Carnegie Mellon University, Pittsburgh, PA, USA
[3]Children's Hospital of Philadelphia, Philadelphia, PA, USA

Abstract

Image processing, virtual anatomy-editing tools, and computational solvers (CFD) offer unique opportunities for pre-operatively modeling and evaluating surgical repairs of congenital heart disease, such as single ventricle defects. In a recent case, three patient-specific Fontan models were evaluated using CFD. To better understand their impact on entire circulation, we extend this work by performing lumped parameter simulations with a circuit analog of the cardiovascular system.

For the relatively small range of resting Fontan resistances evaluated (0.66-1.30 WU), large decreases in cardiac output (12%) and systemic arterial pressure (9%), and a slight increase in mean systemic venous pressure (2%) were observed. In summary, the inclusion of 1D lumped parameter modeling to existing surgical planning methodologies may allow researchers and clinicians to better understand the impact of Fontan hemodynamics on the rest of the body.

1. Introduction

Surgical palliation to address single ventricle congenital lesions commonly results in the formation of the Total Cavopulmonary Connection (TCPC), which is characterized by the direct anastomosis of the systemic veins to the pulmonary arteries [1]. Although this approach has led to significant improvements in postoperative mortality, numerous studies have demonstrated that serious, long-term functional complications, such as ventricular dysfunction, thromboembolism, arrhythmia, or protein-losing enteropathy are common [2,3]. As a result, many researchers have sought to hemodynamically optimize flow through the TCPC via the geometric characteristics of the surgical implementation [4,5]. However, as the modelling efforts have progressed to include patient-specific complexity [6,7], it has become apparent that patient-to-patient anatomical variations give generic guidelines for TCPC design limited utility.

To address this limitation, recent efforts have sought to develop robust virtual anatomy editing tools for the surgical planning of patient-specific cases [8]. In other words, using pre-operative cardiac magnetic resonance (CMR), researchers and clinicians are able to 1) reconstruct the patient-specific anatomy and *in vivo* flow fields, 2) virtually construct the array of available surgical options, and 3) use computational fluid solvers to evaluate the generated options to select the best one. To date, this methodology has been successfully applied in a limited number of clinical cases [9].

One shortcoming of this approach is that the computational solver considers the TCPC in a vacuum, i.e., there is no simulation or direct prediction of the effect of the geometry-related hemodynamics to the rest of the cardiovascular system. Specifically, the relationship between the TCPC flows and the cardiac function are believed to be critical determinants of ultimate patient outcome. Previous studies have developed mathematical models with lumped parameter representations of the entire circulatory system to investigate these connections using physiological average values and ranges [10]. The objective of the present study was to apply such a model to the evaluation of surgical options for a patient-specific case study.

2. Methods

Surgical Planning- For a detailed description of the step-by-step methodology of surgical planning, the reader is referred to [9]. Briefly, the CMR data were segmented and reconstructed to provide the detailed anatomical and boundary flow conditions using in-house programs. State-of-the-art geometrical morphing concepts were then applied through a robust surgical planning interface to generate a number of potential anatomic configurations.

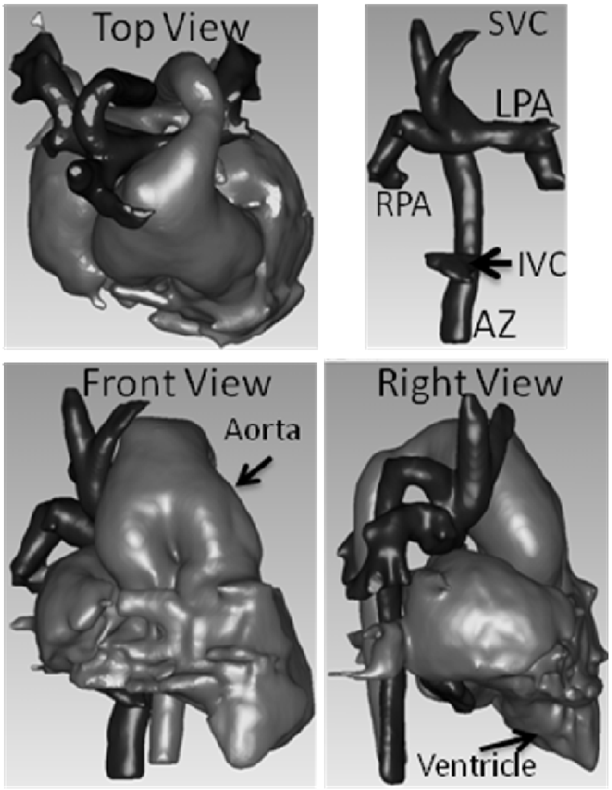

Figure 1. *3D Reconstruction of the patient-specific anatomy (black), including the single ventricle and aorta (light gray). IVC/SVC- inferior/superior vena cava; AZ- azygos vein; RPA/LPA- right/left pulmonary artery.*

Patient Details- The following details and study results pertain to a 3-year-old female patient with Heterotaxy syndrome, an unbalanced atrioventricular canal and interrupted IVC who had previously undergone a Kawashima procedure. She was referred to Children's Hospital of Philadelphia for Fontan completion to alleviate decreasing oxygen saturations (75%) as a result of bilateral pulmonary arteriovenous malformations. The 3D reconstruction of the Kawashima and surrounding anatomical structures is shown in Figure 1.

With the primary objective of evenly distributing blood flow from the IVC to each of the PAs, three surgical planning options were generated and are herein described. In option 1, a lateral tunnel was created from the IVC, through the atrium, and inferiorly connected to the PAs with a slight (~1/2 diameter) offset between the SVC and IVC. For option 2, an extracardiac conduit was routed around the atrium, connecting anteriorly to the PAs with slight preferential curvature toward the LPA. Finally, in option 3, the IVC was simply connected to the azygos vein at the level of the diaphragm. The models for each of these options are shown in Figure 2.

CFD Simulations- In order to predict the resistance values associated with each design, full 3D flow simulations were conducted using an in-house, unstructured, sharp interface immersed-boundary method. Two sets of simulations were conducted per model, with cardiac outputs of 3.85 and 5.85 L/min to emulate the corresponding resting and exercise resistance values, respectively. Simulated resistances for each option are shown in Table 1.

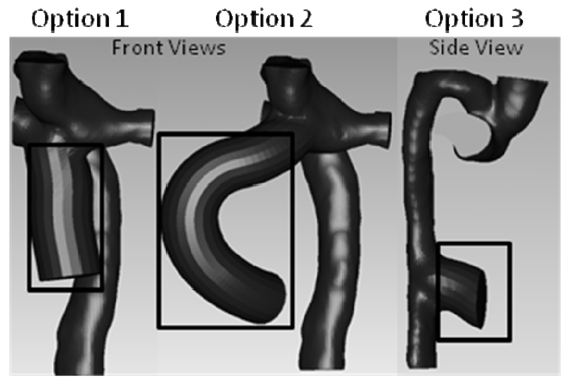

Figure 2. *The three surgical planning models created for the patient; IVC baffle for each is highlighted in the boxed region.*

Lumped Parameter Model- In this analysis, an electrical circuit analog of the cardiovascular system, as described by Sundareswaran et al. [10], was used in which the arteries, veins, and heart chambers were modeled as pure, time-dependent compliance chambers with lumped resistances. To specifically model the Fontan circulation, a chamber representing the lumped TCPC resistance was included between the systemic and pulmonary vascular resistance components, in lieu of a right ventricle. Figure 3 shows a schematic representation of the specific model used in the study.

The instantaneous flow and pressure from compartment i to compartment j were evaluated by iteratively solving the following set of differential equations until convergence (>10 cardiac cycles):

$$Q_{ij} = (P_j - P_i) \times \frac{1}{R_{ij}} \times S_{ij} - \frac{L_{ij} Q_{ij}}{R_{ij}} \times S_{ij}$$
$$\frac{d(C_i P_i)}{dt} = \sum_{j-1}^{N} j(Q_{ij} - Q_{ji}) \qquad (1)$$

P_i, Q_i, and C_i are the pressures, flows, and compliances of chamber i; R_{ij}, L_{ij}, and S_{ij} are the resistances, lumped impedances, and valve switches enforcing directionality between chambers i and j, respectively. Specific values for resistances, with the exception of the CFD-derived TCPC resistance, were obtained from patient-specific catheterization (Table 1). Impedance and compliance values were obtained from literature [11].

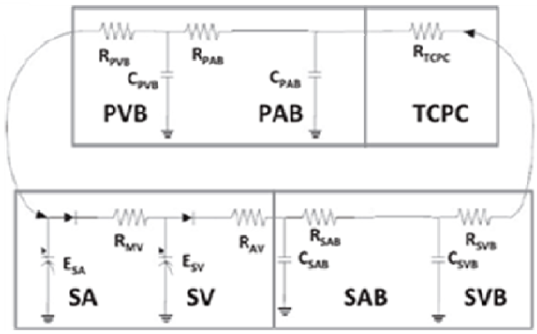

Figure 3. Schematic describing the lumped parameter model used in the study. R- resistance; C- compliance; E- load; PVB- pulmonary venous bed; PAB- pulmonary arterial bed; SA- single atrium; SV- single ventricle; SAB- systemic arterial bed; SVB systemic venous bed; MV- mitral valve; AV- aortic valve.

Table 1. Input parameters to the lumped parameter model

Parameter	**Rest Value**	**Exercise Value**
Cardiac Output	**3.85 L/min**	N/A
Heart Rate	**79 bpm**	150 bpm
SVR	**14.79 WU**	8.87 WU
PVR	**2.19 WU**	1.31 WU
R_{TCPC1}	0.73 WU	1.05 WU
R_{TCPC2}	0.66 WU	1.17 WU
R_{TCPC3}	1.30 WU	2.21 WU

*Numbers shown in bold were obtained from cardiac catheterization. TCPC resistances were obtained from CFD. Exercise values were imposed based on expected physiologic responses seen in literature. Wood Units (WU) are a clinically used resistance measure and are equivalent to mmHg*min/L.*

To drive the cardiac cycle in the simulations, the single ventricle was modeled as a time-varying compliance chamber. The pulsatile pressure profile was thus generated using functions with alternating systolic and diastolic characteristics as follows:

$$E(t)=\frac{1-e^{-t/T_c}}{1-e^{-T_S/T_c}},(0\le t\le T_S)$$
$$CV(t)=CVD\times(CVS/CVD)^{E(t)}$$
$$E(t)=\frac{1-e^{-(t-T_S)/T_r}}{1-e^{-(T-T_S)/T_r}},(T_S\le t\le T) \quad (2)$$
$$CV(t)=CVS\times(CVD/CVS)^{E(t)}$$

E is the load of the ventricle, T_c (0.0025 min) and T_r (0.0075 min) are time constants governing the contraction and relaxation of the muscle during systole and diastole, T is the duration of the cycle (1/heart rate), T_S is the length of systole (T/3 for rest, T/2 for exercise), t is the current point in the cardiac cycle, and CVD and CVS were the maximum and minimum compliance values of the chamber, respectively.

In addition to the baseline conditions from the catheterization data, exercise conditions were simulated for each option. The assumptions made to approximate exercise physiology, as described by Sundareswaran et al. [10], were: 1) increased heart rate, 2) decreased systemic vascular resistance (up to 50%), and 3) decreased pulmonary vascular resistance (up to 40%). In addition, as shown in Table 1, the 3 TCPC resistances increased under exercise due to the increased cardiac output.

To evaluate each of the surgical options under both resting and exercise conditions, the following parameters were measured/obtained from the model output: cardiac output (CO); end systolic pressure (ESP); central venous pressure (CVP); end diastolic pressure (i.e., ventricular preload) (EDP); ventricular afterload (E_a); ventricular contractility (E_{es}); and ventricular-vascular coupling ratio (E_a/E_{es}). The final three parameters were evaluated based on the methodology of Nogaki et al. [12].

3. Results

Results of the model simulations are summarized in Table 2. For resting conditions, it was found that options 1 and 2 approximately maintained the pre-operative cardiac output, whereas option 3, which had the highest resistance value, depressed the output by 12%. Additionally, the coupling ratio, E_a/E_{es}, for options 1 and 2 was found to be near the normal value of 0.42 for the biventricular circulation [12], but abnormally high for 3. CO increased with exercise for all three options, but again, option 3 yielded a significantly lower CO than the others. Also, the coupling ratios were abnormally increased in all cases. Other general trends that were observed include: decreasing ESP and EDP, and increasing CVP and E_a with increasing TCPC resistance.

Table 2.- Summary of lumped parameter results.

	O1rest	O2rest	O3rest	O1ex	O2ex	O3ex
CO	3.82	3.87	3.4	5.26	5.08	3.92
ESP	79	79.9	72.4	67.5	65.8	55
CVP	15.1	15	15.4	15.6	15.7	16.2
EDP	3.47	3.53	3.11	2.55	2.45	1.91
E_a	1.64	1.63	1.68	1.92	1.94	2.1
E_{es}	3.53	3.56	3.27	3.06	3.00	2.54
E_a/E_{es}	0.46	0.46	0.51	0.63	0.65	0.83

4. Discussion and conclusions

In their previous study, Sundareswaran et al. demonstrated the impact of TCPC geometry and hemodynamics on cardiac function using a cohort of 16 patients and averaged resistance values. The present study corroborates and extends that work by similarly demonstrating importance of TCPC design in a single patient using all patient-specific cardiovascular measures. Specifically, it was seen that a TCPC design with elevated resistance (option 3) had drastically negative effects on the cardiac output, ventricular preload and afterload, as well as ventricular-vascular coupling. Furthermore, while the first two options produced resting values that appeared to be within acceptable physiologic ranges, the exercise simulations revealed that they were still far from ideal solutions. In fact, for all three exercise simulations, the cardiac function was not able to properly meet the demand of the body for increased output, as denoted by the altered coupling ratio, i.e., the afterload was increasing faster than the ventricular contractility, resulting in decreased systemic pressures.

The results of this study also emphasize the importance of surgical planning and multi-parameter patient-specific modelling in complex congenital heart disease. As previously mentioned, the primary objective of the surgical intervention in this case was to ensure even distribution of IVC blood flow. The CFD results (not shown here) indicated that options 1 and 3 satisfied that objective with near 60/40 distributions. However, considering the energy characteristics of those connections and their effect on the rest of the body revealed that option 1 was clearly superior. Without the assistance of the fluid solver and mathematical model, the surgeon would have been lacking these valuable insights. Furthermore, it is worth noting that the IVC-to-Azygos connection (option 3) was selected as the optimal configuration for the case study presented by Sundareswaran and de Zelicourt et al. [9]; whereas, it was found to be inferior for the present patient, thus further underscoring the need for patient-specific models.

Finally, despite the achievement of mathematical convergence in the simulations, the physiologic state, as presented here, is not in equilibrium because the CFD solver and lumped parameter model are decoupled. For example, the exercise resistance values were obtained assuming a flow rate of 5.85 L/min for the CFD boundary conditions; however, as the results indicate, the modelled flow rates failed to reach that level. Thus, the actual resistances would have been slightly lower and the flow rates higher, but the actual solution would have been therefore bounded by the resistances tested and, more importantly, the relative differences between options would be obviously unaffected. Nonetheless, steps should be taken to couple these tools to improve the accuracy and applicability of both.

In summary, a lumped parameter mathematical model was used to assess the impact of resistance values for individual TCPC surgical options. It was shown that differences in design within a single patient could lead to vastly different states of global cardiac function, emphasizing the importance of a patient-specific approach and the utility of advanced surgical planning tools in the treatment of single ventricle patients.

Acknowledgements

This work was funded by National Heart, Lung, and Blood Institute Grant HL-67622.

References

[1] de Leval MR, Kilner P, Gewillig M, Bull C. Total cavopulmonary connection: A logical alternative to atriopulmonary connection for complex Fontan operations. Journal of Thoracic and Cardiovascular Surgery. 1988;96(5):682-95.

[2] Gersony DR, Gersony WM. Management of the postoperative Fontan patient. Progress in Pediatric Cardiology. 2003;17:73-9.

[3] McCrindle BW, Williams RV, Mitchell PD, Hsu DT, et al. Relationship of Patient and Medical Characteristics to Health Status in Children and Adolescents after the Fontan Procedure. Circulation. 2006;113:1123-9.

[4] Sharma S, Goudy S, Walker P, Panchal S, et al. In Vitro Flow Experiments for Determination of Optimal Geometry of Total Cavopulmonary Connection for Surgical Repair of Children with Functional Single Ventricle. Journal of the American College of Cardiology. 1996;27(5):1264-9.

[5] Soerensen DD, Pekkan K, et al. Introduction of a New Optimized Total Cavopulmonary Connection. Annals of Thoracic Surgery. 2007;83:2182-90.

[6] de Zelicourt DA, Pekkan K, Wills L, Kanter K, et al. In Vitro Flow Analysis of a Patient-Specific Intraatrial Total Cavopulmonary Connection. Annals of Thoracic Surgery. 2005;79:2094-102.

[7] de Zelicourt D, Pekkan K, Parks WJ, Kanter K, Fogel M, Yoganathan AP. Flow study of an extracardiac connection with persistent left superior vena cava. Journal of Thoracic and Cardiovascular Surgery. 2006;131:785-91.

[8] Pekkan K, Whited B, Kanter K, et al. Patient-specific surgical planning and hemodynamic computational fluid dynamics optimization through free-form haptic anatomy editing tool (SURGEM). Medical and Biological Engineering and Computing. 2008;46(11):1139-52.

[9] Sundareswaran KS, de Zelicourt D, Sharma S, Kanter K, Spray TL, Rossignac J, et al. Correction of Pulmonary Arteriovenous Malformation Using Image-Based Surgical Planning. Journal of the American College of Cardiology: Cardiovascular Imaging. 2009;2(8):1024-30.

[10] Sundareswaran KS, Pekkan K, Dasi LP, et al. The total cavopulmonary connection resistance: a significant impact on single ventricle hemodynamics at rest and exercise. American Journal of Physiology Heart and Circulatory Physiology. 2008;295:H2427-H35.

[11] Peskin CS, Tu C. Hemodynamics in Congenital Heart Disease. Computers in Biology and Medicine. 1986;16(5):331-59.

[12] Nogaki M, Senzaki H, Masutani S, et al. Ventricular energetics in Fontan circulation: Evaluation with a theoretical model. Pediatrics International. 2000;42:651-7.

Address for correspondence:
A.P. Yoganathan
Georgia Institute of Technology
313 Ferst Dr., Atlanta, GA 30332-0535
ajit.yoganathan@bme.gatech.edu